

## **PERMSELECTIVITY AND STRUCTURE PROPERTIES OF ETHYLENE-CO-VINYL-ACETATE MEMBRANES HYDROLYSED WITH DIFFERENT TIMES**

*E. Bureau<sup>1</sup>, Y. Hirata<sup>2</sup>, C. Cabot<sup>1</sup>, A. Andrio Balado<sup>3</sup>, S. Marais<sup>2\*</sup> and J. M. Saiter<sup>1</sup>*

<sup>1</sup>Laboratoire d'Etudes et de Caractérisation des Amorphes et des Polymères, Université de Rouen, UFR des Sciences, 76821 Mont-Saint-Aignan Cedex, France

<sup>2</sup>Laboratoire 'Polymères, Biopolymères, Membranes', UMR6522, Université de Rouen/CNRS, UFR des Sciences, 76821 Mont-Saint-Aignan Cedex, France

<sup>3</sup>Department of Experimental Science, Universitat Jaume I, Castelló 12080, Spain

### **Abstract**

In this work, the influence of a unilateral hydrolysis treatment on O<sub>2</sub> and H<sub>2</sub>O permeation properties of poly(ethylene-co-vinyl acetate) (EVA) containing 70 mass% of vinyl acetate are investigated. On the one hand, the O<sub>2</sub> permeability decreases with the reaction time (0 to 16 h), while the H<sub>2</sub>O permeability passes through a maximum for a hydrolysis of 30 min. On the other hand, the existence of structural changes as a function of the hydrolysis duration is checked by means of DSC investigations. Results lead to conclude that a crystalline phase occurs by hydrolysis and is responsible of the permeation changes.

**Keywords:** crystallinity, DSC, hydrolysis, permeability, permeation, poly(ethylene-co-vinyl acetate)

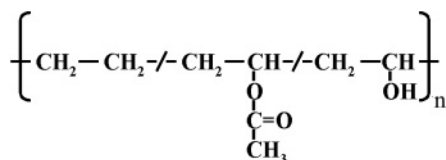
### **Introduction**

Barrier properties for packaging materials have been improved in recent years and the films protecting foods from oxidation and moisture that perform well are poly(ethylene terephthalate), polyethylene, polypropylene, and poly(vinylidene chloride), etc. Completely hydrolyzed poly(ethylene-co-vinyl acetate) (EVA), leading to poly(ethylene-co-vinyl alcohol), is one of the least permeable polymers in the dry state. Its perfect gas barrier properties for water and oxygen, however, are not suitable for fresh fruits and vegetables. These foods are perishable and need protective packaging until they are used. During the period of preservation they produce biochemical reactions that consume oxygen and yield carbon dioxide and water. There is a trade-off between the respiratory intensity and the period of their preservation. By reducing the partial pressure of oxygen in the packaging materials the respiratory intensity can be reduced so that the product lasts longer. Moreover, the condensation of water gener-

\* Author for correspondence: E-mail: stephane.marais@univ-rouen.fr

ated by the biochemical reactions induces moulds, and also the anaerobic fermentation of bio-components under high water and CO<sub>2</sub> contents often leads to a bad taste and smell. For a better preservation of fresh fruits and vegetables, it is necessary to increase the water permeability and keep the permeability for oxygen low in order to reduce the respiratory intensity and the anaerobic fermentation rate.

From these considerations, the aim of this study was to prepare membranes exhibiting high H<sub>2</sub>O/O<sub>2</sub> permselectivities. We have reported that the H<sub>2</sub>O/O<sub>2</sub> permselectivities of membranes of copolymers of ethylene with vinyl acetate increase with the vinyl acetate contents (from 2 to 70 mass%) [1]. In order to improve their permselectivities, pseudo 'bi-layer' membranes, based on EVA containing 70 mass% of vinyl acetate groups, were prepared by unilateral hydrolysis using solutions of sodium hydroxide in a mixture of water and methanol. So, 'bi-layer' membranes are formed by a first homogenous layer of EVA and a second heterogeneous layer of hydrolyzed EVA. Thus, the chemical structure of the treated layer is composed of poly(ethylene-co-vinyl acetate-co-vinyl alcohol).



Scheme 1

The depth of the hydrolyzed layers and the concentration of hydroxyl groups in the EVA membranes were controlled by the treatment time in the solutions and were characterized by means of IR spectroscopy and fluorescent microscopy. The transport properties of water and oxygen through the 'bi-layer' membranes were studied by permeation measurements. In order to investigate the structure-property relationships in greater depth, the influence of the hydrolysis treatment was investigated by DSC experiments.

## Experimental

### *Polymer film preparation*

Poly(ethylene-co-vinyl acetate) (EVA) containing 70 mass% of vinyl acetate was of the Baymod type, kindly provided by Bayer Corp. Dense films of EVA were prepared by casting from dichloromethane (10 mass%) solutions onto a glass plate. The film obtained was dried for 12 h under atmospheric pressure at room temperature and then dried in an oven for 7 h at 80°C. After cooling at room temperature, the edges of the films were turned up to form a 'boat' measuring 130 mm by 150 mm, this was left on the glass plate. A 120 mL solution of a 0.8 molar NaOH and containing 75 vol.% of methanol and 25 vol.% of water was spread in the 'boat'. Different hydrolysis times, from 30 min to 16 h, were used. The reaction was terminated by adding 150 mL of an aqueous 3.0 M HCl solution. After 15 min, the films were soaked in water for two days to remove HCl until pH=7 was reached. Finally, they were removed from the glass plate and transferred

first to polyethylene sheets, with the non-treated side facing the polyethylene; they were then exposed to the air for 24 h before being dried over  $P_2O_5$  in a desiccator at room temperature under vacuum for 24 h. The film thickness was approximately 150  $\mu\text{m}$ . In order to estimate the depth of the hydrolyzed layer of the membranes, the cross-section view of the membranes, dyed with Rhodamine 6G (Aldrich), was observed by optical microscopy using fluorescent light. The fluorescence of the two dyed layers, was observed but with different intensities due to the difference in solubility of Rhodamine 6G between the modified and the unmodified layers. Prior to the observation, the membranes were treated as follows: Rhodamine 6G was dissolved in a methanol solution containing 25 vol.% of water. The membranes were stored in the solution for 24 h and then were rinsed until the water was clear. After drying, the dyed membranes were used only for fluorescence light.

#### *Permeation measurement*

The water and oxygen permeabilities of the membranes were measured using two complementary hygrometric sensors (chilled mirror and capacitive hygrometers) and an oxymeter analyzer according to the experimental method developed by Marais *et al.* [2]. The method and procedure are explained in a previous publication [3]. Oxygen permeability is determined from dried samples, so that the permeation measurements (water and oxygen) are performed with the same material but not at the same state. The difficulty in our permeation process is the fact that to measure very low fluxes of gases, our permea-diffusiometer (differential permeation) is limited and the time-lag permeation is then used but is unable to give a specific response for a mixture of gas and water. This is why in this paper the comparison of permeabilities is given for pure permeants.

#### *DSC experiments*

Calorimetric measurements were carried out with a 2920 modulated DSC (Thermal Analysis instrument) equipped with a low temperature cell (minimal temperature =  $-50^\circ\text{C}$ ). The temperature was scanned from  $-50$  to  $180^\circ\text{C}$  in the standard mode with a constant heating rate of  $5\text{ K min}^{-1}$ . Calibrations for both the temperature and the enthalpy were achieved from measurements of melting temperature and enthalpy of indium ( $T_m = 156.6^\circ\text{C}$  and  $\Delta H_m = 28.45\text{ J g}^{-1}$ ). The mass of the samples was about 15 mg, encapsulated in standard DSC aluminium pans. Experiments were performed under a neutral nitrogen atmosphere. Before experiments, samples were stored in a vacuum desiccators over  $P_2O_5$  for at least two weeks to avoid moisture sorption effects.

#### *IR spectroscopy*

The IR spectra were obtained by using ATR method (Attenuated total reflection), and by collecting and averaging 32 scans, at a resolution of  $4\text{ cm}^{-1}$ .

## Results and discussion

### 'Pseudo bi-layer' membranes

The attenuated total reflection (ATR) spectrum reflects the average surface structure of the materials in limited depth (1 to 4  $\mu\text{m}$ ). The ATR method does not give information about the total amount of functional groups in the samples. However, this method permits the comparison between the treated and the untreated surface structures of the membranes. Figure 1 shows the hydrolysis degree of the hydrolyzed and untreated surface layers of the membranes. In the EVA membrane, the  $1730\text{ cm}^{-1}$  band was attributed to the carbonyl group due to the vinyl acetate structure. The relative intensities of carbonyl group normalized with the peak area of the carbonyl group of EVA membrane,  $A_{1730}/A_{1730(\text{EVA})}$  are plotted. It can be observed that for the treated surfaces of the membranes, the relative intensity decreases as the reaction time increases while, for the untreated surfaces, the relative intensity is not changed up to 3 h of the reaction time, after which, it decreases. This observation indicates that the EVA layer exists at the untreated side of the membranes for which the reaction time is less than 3 h, and the membranes treated for more than 4 h have a gradient of hydrolysis in all the thickness.

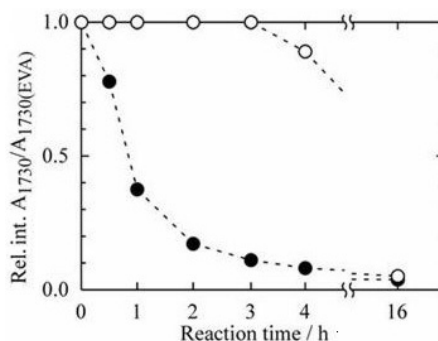


**Fig. 1** Hydrolysis degree of the surface vs. reaction time from ATR-mode FTIR spectra; ● – hydrolyzed and ○ – non-treated surfaces

The attenuated total reflection (ATR) spectrum and the fluorescent microscopy confirmed that all the membranes used in this study have two layers [4].

In the EVA membrane, the  $1730\text{ cm}^{-1}$  band was attributed to the carbonyl group due to the vinyl acetate structure. The relative intensities of the carbonyl group for the untreated surfaces, which are normalized with the peak area of the carbonyl group of the EVA membrane,  $A_{1730}/A_{1730(\text{EVA})}$ , do not change for the first 3 h of the reaction time, after which, they decrease. The hydrolyzed layers of the EVA membranes that are treated from 30 min to 3 h expand from 27 to 80  $\mu\text{m}$  with the reaction time [3].

When the reaction time is less than 3 h, no modification is detected on the EVA layer at the untreated side of the membrane. For those membranes treated for more than 4 h, however, a gradient of hydrolysis across the entire membrane thickness appears.

Examination of the specimen surface by the ATR spectra and the fluorescent microscopic reveals that the membranes after unilateral hydrolysis are asymmetric and are characterized by different depth of hydrolyzed layers and different concentration of hydroxyl groups.

*Dependence of oxygen and water transport properties on the reaction time*

We have previously reported that a different tendency of the water permeation through the pseudo ‘bi-layer’ membranes is observed compared to oxygen permeation [5]. As shown in Fig. 2, the permeability coefficients for oxygen in the pseudo ‘bi-layer’ membranes decrease with reaction time, while the permeability coefficients for water through the membranes hydrolyzed for 30 min ( $P=9.8 \cdot 10^{-7} \text{ cm}^3 \text{ (STP) cm cm}^{-2} \text{ s}^{-1} \text{ cmHg}^{-1}$ ) and 1 h ( $P=8.9 \cdot 10^{-7} \text{ cm}^3 \text{ (STP) cm cm}^{-2} \text{ s}^{-1} \text{ cmHg}^{-1}$ ) are slightly greater than that of the EVA70 membrane ( $P=8.6 \cdot 10^{-7} \text{ cm}^3 \text{ (STP) cm cm}^{-2} \text{ s}^{-1} \text{ cmHg}^{-1}$ ). These differences are significant since the measurement accuracy is good (error<4%). After 2 h of treatment, the water permeability significantly decreases as a function of the reaction time. The permeation behavior for small molecules through the membranes can be explained by solution-diffusion model as follows [5, 6]:

$$P=DS \quad (1)$$

The diffusion and solubility coefficients for  $\text{H}_2\text{O}$  and  $\text{O}_2$  in the EVA membranes before and after unilateral hydrolysis are shown in Figs 3 and 4. The diffusion coefficients were calculated using the time lag  $t_L$  [2, 7]. Dividing  $P$  by  $D$  gives  $S$ . These parameters for the pseudo ‘bi-layer’ membranes of the different reaction times are apparent values because these membranes are asymmetric in the direction of permeation as mentioned previously.

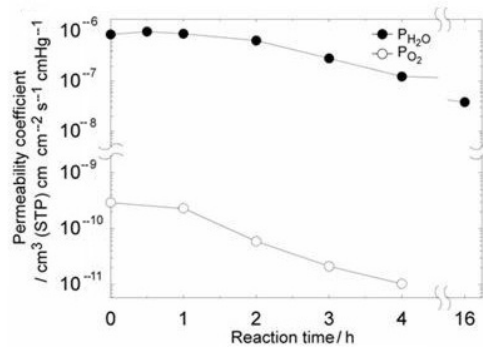


**Fig. 2** Permeability coefficients for  $\text{O}_2$  and  $\text{H}_2\text{O}$  vs. hydrolysis time of EVA membranes

The diffusion coefficients for both water and oxygen permeants in the ‘bi-layer’ membranes decrease with reaction time. The solubility coefficients of oxygen in the ‘bi-layer’ membranes decrease with reaction time while the solubility coefficients of water increase with reaction time. The hydrolyzed layers in the pseudo ‘bi-layer’

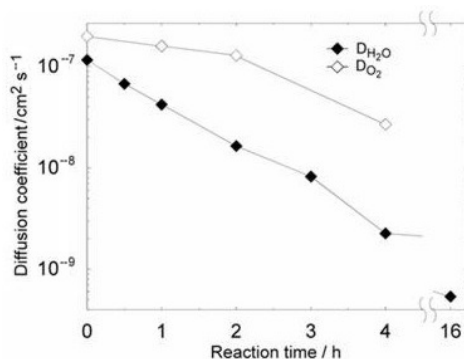


Fig. 3 Diffusion coefficients for O<sub>2</sub> and H<sub>2</sub>O vs. hydrolysis reaction time of EVA membranes

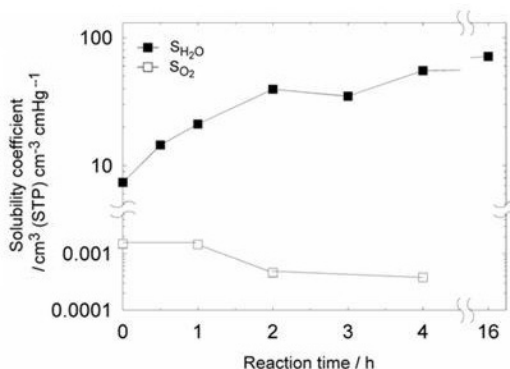


Fig. 4 Solubility coefficients for O<sub>2</sub> and H<sub>2</sub>O vs. hydrolysis reaction time of EVA membranes

membranes contain the hydroxyl group of vinyl alcohol so it must be kept in mind that each hydroxyl group is bound by inter- and intra-hydrogen bonds.

#### Structural properties of hydrolyzed EVA membranes

DSC experiments were used to study the influence of hydrolysis reaction time on EVA70 membrane morphology and to correlate its variation with permeation properties. Figure 5 shows the results of DSC measurements on all samples (from non-treated EVA70 to EVA70 hydrolyzed during 16 h).

The enthalpic curve of the non-hydrolyzed sample is characteristic of wholly amorphous material and an endothermic step due to the glass transition at  $T_g = -20^\circ\text{C}$  can be observed ( $T_g$  being defined as the midpoint glass transition temperature). The variation of heat capacity  $\Delta C_p$  occurring at the glass transition temperature  $T_g$  is defined by

$$\Delta C_p = (C_{p,l} - C_{p,g})_{T=T_g} \quad (2)$$

where  $C_{p,l}$  is the specific thermal heat capacity in the liquid-like state and  $C_{p,g}$  is the thermal heat capacity in the glassy state.  $\Delta C_p$  is equal to  $(0.56 \pm 0.05) \text{ J g}^{-1} \text{ K}^{-1}$ .

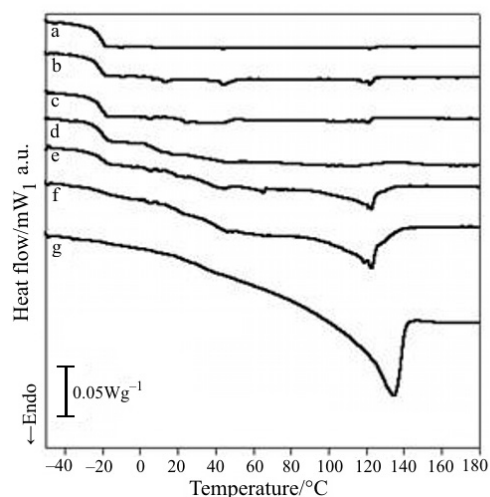


**Fig. 5** DSC curves a – non-treated, b – 30 min, c – 1 h, d – 2 h, e – 3 h, f – 4 h and g – 16 h

For hydrolyzed samples, DSC experiments show how the structure evolves with the hydrolysis duration. On the one hand, a constant position of the glass transition characteristic of amorphous EVA is observed (Fig. 5), and this is followed by a reduction in ‘intensity’  $\Delta C_p$ . On the other hand, an endothermic peak appears (around 130°C) progressively with the hydrolysis duration. This peak corresponds to the melting of a crystalline phase present in the material. Clearly, the degree of crystallinity (DoC) increases with the hydrolysis time, and this DoC is proportional to the melting enthalpy  $\Delta H_m$  obtained from the area of the endothermic phenomena appearing between 0 and 150°C. Melting temperature  $T_m$  (at the maximum of the peak), melting enthalpy  $\Delta H_m$ , glass transition temperature  $T_g$  and heat capacity variation  $\Delta C_p$  are reported in Table 1 for all materials.

**Table 1** Values of  $T_g$ ,  $\Delta C_p$ ,  $T_m$  and  $\Delta H_m$  vs. reaction hydrolysis time  $t_h$

| $t_h/h$ | $T_g/^\circ\text{C}$ | $\Delta C_p/\text{J g}^{-1} \text{K}^{-1}$ | $T_m/^\circ\text{C}$ | $\Delta H_m/\text{J g}^{-1}$ |
|---------|----------------------|--|----------------------|------------------------------|
| 0       | -20                  | 0.56                                       | –                    | 0                            |
| 0.5     | -20.5                | 0.49                                       | –                    | 4                            |
| 1       | -20.5                | 0.56                                       | –                    | 2                            |
| 2       | -20                  | 0.37                                       | –                    | 14                           |
| 3       | -19.5                | 0.34                                       | 122                  | 36                           |
| 4       | -19                  | 0.18                                       | 122                  | 63                           |
| 16      | –                    | –  | 135                  | 84                           |

Figure 6 shows the variations of the  $\Delta C_p$  and  $\Delta H_m$  with the hydrolysis time  $t_h$ . Between 0 and 1 h, there is practically no significant variation of the morphology. It

seems that the membranes are wholly amorphous in this range of time while hydroxyl groups are created in the treated layers. This can be linked to the phenomena observed for the permeation properties: no significant change for oxygen permeation and a maximum value at 30 min for water permeation. Between 1 and 7 h, we observe, first, a drastic decrease of the  $\Delta C_p$  value, characterizing a reduction in proportion of amorphous phase, and then vanishing for  $t_h > 7$  h. This is confirmed by the plot showing the evolution of  $\Delta H_m$  with time: a drastic increase of  $\Delta H_m$ , in the same time range, is observed. A crystalline phase appears and grows with hydrolysis treatment. This crystalline phase growing with reaction time can explain the decreasing evolution of the permeation properties of oxygen and water in EVA70.

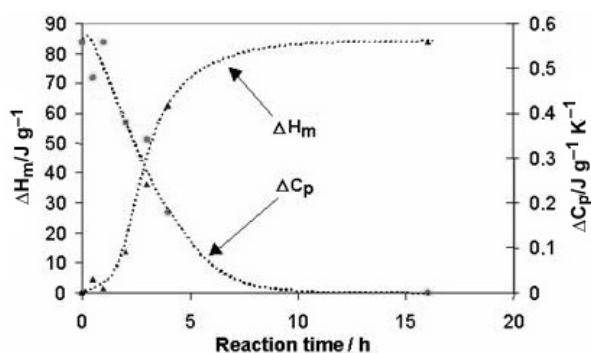


**Fig. 6** Plots of melting enthalpy  $\Delta H_m$  and heat capacity variation  $\Delta C_p$  vs. duration of hydrolysis of the EVA membranes

The results of DSC experiments show that two crystalline phases originating from both polyethylene and poly(vinyl alcohol) units are reorganized during hydrolysis. It is well-known that poly(vinyl alcohol) has a crystalline region stabilized by hydrogen bond [8]. These crystalline regions are not observed in the EVA membrane which is completely amorphous. The oxygen molecules are insoluble in the crystalline regions in polymers [9], which means the regions act as impermeable barriers analogous to filler particles [10]. We conclude that increasing crystallinity reduced both diffusivity and solubility for oxygen in the 'pseudo bi-layer' membranes. In the case of water, solubility increased with the reaction time though the diffusivity decreased. It is thought that the crystalline region originating from polyethylene units is not destroyed by water molecules but the hydrogen bond between the hydroxyl groups in the amorphous or crystalline regions can be cut by water penetration. Using the sorption isotherm of water in the pseudo 'bi-layer' membranes, we have previously found that the concentration of hydroxyl groups increases as the reaction time rises and the solubility of water and the insufficiently plasticized layers act as an obstacle to the diffusion of water molecules along the hydrogen bond between hydroxyl groups; this is because of the gradients of water concentration in membranes in the permeation experiment [5]. When the concentration of the hydroxyl groups is low, it seems that each hydroxyl group is dispersed in the materials. The increase in the concentration of the hydroxyl groups caused the rearrangement of polymer chains be-



cause of the large difference of polarity between polyethylene and poly(vinyl alcohol) units in this study. It is concluded that the hydroxyl groups in isolation easily increase the water solubility and facilitate the plasticization effect, while the aggregation of the hydroxyl groups such as the crystalline region is not efficient for the enhancement of both diffusivity and solubility of water. Consequently, the maximum water permeability of the EVA membrane treated for 30 min, compared with the other EVA membranes, is due to the relative increase of its water solubility exceeding the decrease of its water diffusivity.

In this work, the permeation results are correlated with the crystallinity but not with the glass transition temperature. Indeed, the very small increase of the  $T_g$  values with the increase of the hydrolysed EVA ratio is not significantly sufficient to be discussed with the permeometric parameters, knowing that usually the increase of  $T_g$  leads to a reduction of the diffusivity. However, to have a better fundamental approach, it should be interesting to measure the  $T_g$  of the final product, i.e. when the material is plasticized by water. It is well-known that the plasticization phenomenon leads to a decrease of the  $T_g$  that can favour the mobility of the permeant molecules. Concerning the EVA layer, it has been shown that humidity does not affect the oxygen permeability [11] while this is not the case in the EVOH layer (hydrolysed part of EVA) because of the plasticization phenomenon.

## Conclusions

The selectivity of water to oxygen through unilateral hydrolyzed EVA membranes have been studied by permeation measurements. Depending on the hydrolysis time, it was found that the hydrolyzed layers of the 'bi-layer' membranes act as an obstacle to the diffusion and solution of oxygen molecules through the presence of hydrogen bonds between hydroxyl groups. In the case of the EVA membranes treated for 30 min and 1 h, which have the thinnest hydrolyzed layers, the water permeability is improved by the interaction between water molecules and hydroxyl groups. The water permeabilities of the other 'bi-layer' membranes were lower than that of the EVA membrane. DSC measurements showed the presence of crystalline phases due to polyethylene and poly(vinyl-alcohol) units which are responsible for the decrease of  $D$ . The unilateral hydrolysis of the EVA membrane allows to control the selectivity of water to oxygen.

## References

- 1 S. Marais, Q. T. Nguyen, D. Langevin and M. Métayer, *Macro. Symp.*, 175 (2001) 329.
- 2 S. Marais, M. Métayer and M. Labbé, *J. Appl. Polym. Sci.*, 74 (1999) 3380.
- 3 E. Bureau, Y. Hirata, C. Cabot, S. Marais, J. M. Saiter and A. Hamou, *Materials Research Innovations*, accepted.
- 4 Y. Hirata, S. Marais, Q. T. Nguyen and M. Métayer, *Macro. Symp.*, accepted.
- 5 S. Pauly, *Handbook of Polymers* Brandrup J., Immergut EH Wiley-Intersciences (Ed.), New York 1969, Chapter 6, p. 435.

- 6 B. D. Freeman, *Macro.*, 32 (1999) 375.
- 7 H. L. Frisch, *J. Polym. Sci.*, 61 (1957) 93.
- 8 R. M. Hodge, G. H. Edward and G. P. Simon, *Polymer*, 37 (1996) 1371.
- 9 J. Crank and G. S. Park, *Diffusion in polymers*, Academic Press, London and New York 1968.
- 10 D. R. Paul, *Ber. Bunsenges. Phys. Chem.*, 83 (1979) 294.
- 11 S. Marais, J. M. Saiter, C. Devallencourt, Q. T. Nguyen and M. Métayer, *Polym. Testing*, 21 (2002) 425.